54th AIAA Aerospace Sciences Meeting
4 - 8 Jan 2016, San Diego, CA
AIAA-2016-1120

Turbulence Amplitude Modulation in an Externally Forced, Subsonic Turbulent Boundary Layer

Piyush Ranade[1], Subrahmanyam Duvvuri[2], Beverley McKeon[3], Stanislav Gordeyev[4], Kenneth Christensen[5], Eric Jumper[6]
University of Notre Dame, Notre Dame, IN, 46556

This paper describes an experiment in which a forced shear layer external to a turbulent boundary layer is used to impart external large-scale forcing to the boundary layer. The shear-layer forcing creates periodic coherent vortical structures in the shear layer that convect at the shear-layer convective velocity. The convecting coherent structures create a concomitant unsteady pressure field that provides a disturbance for the turbulent boundary layer on the upper wall of the tunnel above the forced shear layer. The unsteady pressure field in turn creates a variation of the effective freestream velocity experienced by the boundary layer, and both the pressure disturbance and the concomitant velocity fluctuations are reported. The character of the turbulence in the boundary layer due to the external forcing is studied through hot-wire anemometry. Thorough examination of the turbulence results in similarities between the turbulence amplitude modulation results due to these externally-forced experiments and modulation response of an internally-forced boundary layer done by others.

I. Introduction

The phenomenon of turbulence "bursting" within a turbulent boundary layer has been studied since the late 1960s [1], with improvements in experimental techniques allowing for a more thorough understanding of the physics of fluid motions and coherent structures in the near-wall region. Most of the work on this subject matter has involved studying a canonical zero pressure-gradient turbulent boundary layer, and understanding the "bursting" through interactions between the large scales of the outer boundary layer and the small scales in the inner layer. The concept of dynamic roughness excitation of a synthetic large scale was first introduced in Jacobi & McKeon [2] and expanded upon by Duvvuri and McKeon [3], who introduced an artificial large scale disturbance into the flow to study its interaction with the small scales in the boundary layer. In this paper, the turbulent boundary layer forming on the upper wall of a shear layer wind tunnel facility was studied. The shear layer formed by the mixing of two parallel streams was mechanically forced to create deterministic large scale vortical structures in the mixing layer. The large coherent structures in the shear layer produced a concomitant unsteady pressure field, which in turn produced a variation of the effective freestream velocity experienced by the boundary layer influencing both the large and small scale structures in the boundary layer. This paper examines the response of the boundary layer structures to the external forcing using hot wire anemometry.

[1] Graduate Student, Department of Mechanical and Aerospace Engineering, Hessert Laboratory for Aerospace Research, Notre Dame, IN 46556, AIAA Student Member.
[2] Graduate Student, Graduate Aerospace Laboratories, California Institute of Technology, Pasadena, CA 91125, AIAA Student Member.
[3] Professor, Graduate Aerospace Laboratories, California Institute of Technology, Pasadena, CA 91125 AIAA Associate Fellow
[4] Research Associate Professor, Department of Mechanical and Aerospace Engineering, Hessert Laboratory for Aerospace Research, Notre Dame, IN 46556, AIAA Associate Fellow.
[5] Professor, Department of Mechanical and Aerospace Engineering, Hessert Laboratory for Aerospace Research, Notre Dame, IN 46556, AIAA Associate Fellow.
[6] Roth-Gibson Professor, Department of Mechanical and Aerospace Engineering, Hessert Laboratory for Aerospace Research, Notre Dame, IN 46556, AIAA Fellow.

Bandyopadhyay and Hussain [4] quantified the relationship between the small and large scales within turbulent boundary layers using a correlation coefficient to correlate the low-frequency (large-scale) component of the fluctuating velocity signal with the high-frequency (small-scale) component. Their experiments revealed a positive correlation close to the wall, intermediate correlation in the log region, and a negative correlation (phase reversal) in the wake region and further away from the wall, indicating a definitive relationship between the large and small scales. This same trend was seen by Hutchins et al.[5] and Mathis et al. [5,6], who introduced the idea of amplitude modulation of the small scales by the large scales, suggesting that the small scale structures reside within the footprint of the large-scale superstructures. The trend was also observed by Duvvuri and McKeon [3] while studying the effect of introducing an artificial large scale.

The work presented in this paper continues to study the relationship between the artificial large scale disturbances created by the unsteady pressure field concomitant with the coherent structures produced in the forced shear layer and small scales in the turbulent boundary layer. While similar to the Duvvuri and McKeon artificial disturbance [3], the shear layer creates a forcing external to the boundary layer instead of the Duvvuri and McKeon experiment, which used disturbances internal to the boundary layer by an oscillating wall surface roughness element. The results indicate a relationship between the artificial large scale and the small scales, possibly suggesting the universality of the amplitude modulation effect.

II. Experimental Setup

The compressible free shear layer facility (CSLF) located in the Hessert Laboratory for Aerospace Research at the University of Notre Dame was used to conduct the experiments described in this paper. The facility is an in-draft facility, and the air is drawn from within the room. Thus, the room total pressure and total temperature define the flow conditions at the inlet. The wind tunnel consists of two inlets, one for the high-speed flow and one for the low-speed flow. The high speed square inlet has a 48.5-to-1 area contraction nozzle that reduces the area from 655.2 in.^{2} to 13.5 in.^{2}, while the low-speed rectangular inlet features a slight expansion from 24.375 in.^{2} to 42.75 in.^{2}. The two flows are separated by a splitter plate located 3 in. from the upper wall. The static pressure of the flows is matched at the splitter plate through the use of densely packed straws arranged streamwise in the expanding low-speed inlet region. The CSLF is pictured in Figure 1.

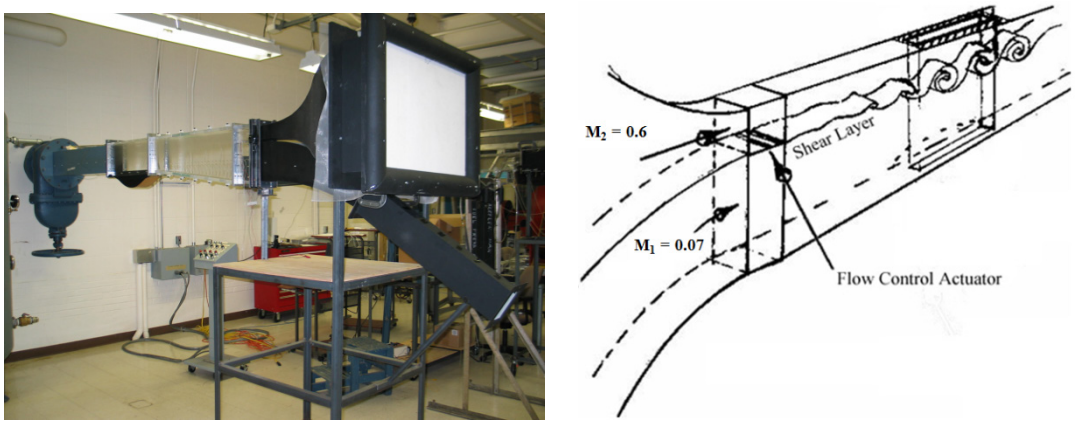

Figure 1: Compressible Shear Layer Facility, photograph (left) and schematic (right).

The mixed flow goes through a throat, and the mass flow rate through the wind tunnel can be adjusted by adjusting the height of the sonic throat. The flow finally exits through a diffuser section, which is connected to one of three openings which lead to a vacuum manifold. The vacuum is produced using two Dekker Magna-Flo vacuum pumps which can be operated individually or together. To eliminate pressure disturbances from the vacuum pumps, the airflow is choked at the throat so that the disturbances cannot propagate upstream of the throat. All of the experiments in this paper are done using a Mach 0.6/0.07 shear layer, since the reliability of hot-wires above Mach 0.6 is questionable.

The amplitude modulation of turbulent structures in the outer region of the boundary layer in this specific facility was first optically observed by Duffin [7] in a separate experiment intended to study the aero-optic effects of the shear layer. The apparent modulation was clearly visible in the optical wavefronts of a laser propagated through

both the shear layer and boundary layer, and Duffin connected its occurrence to the passing of coherent structres. Since the primary focus of Duffin's work involved the shear layer, the modulation in the boundary layer was left as an open question, which motivated the work reported in this paper. The optical experiments had been performed at a streamwise distance of x = 0.43 m, and thus for the sake of comparison, this location was chosen to conduct hot-wire and unsteady pressure experiments. Following the work of Duffin [7], the Mach 0.6/0.07 shear layer was forced using voice-coil actuators on the splitter plate at a frequency of 675 Hz. A sub-harmonic at half of the forcing frequency and one-tenth amplitude was added to the forcing signal to control the vortex pairing mechanism which serves to regularize the shear layer. The voice coil actuators and the forcing signal are shown in Figure 2.

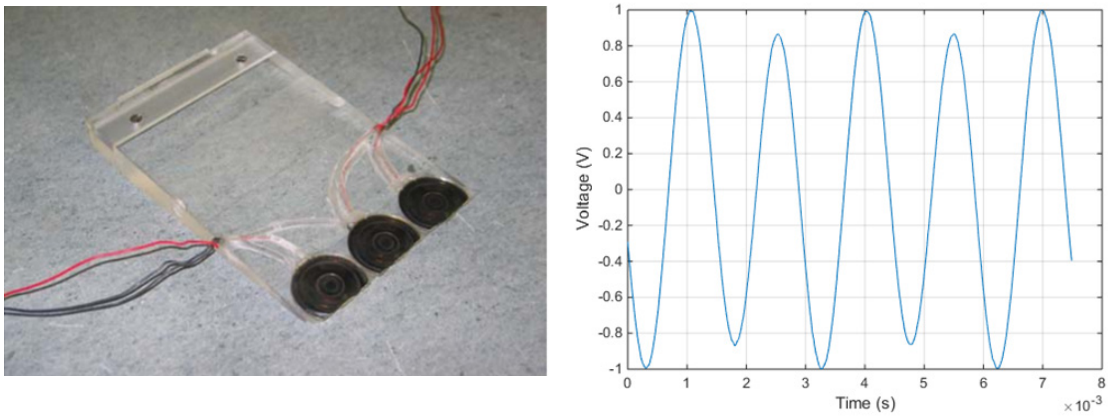

Figure 2: Photograph of voice coil actuators on splitter plate (left), and forcing signal (right)

A Dantec single-wire miniature boundary-layer hot-wire probe was used to acquire time series of velocity throughout the boundary layer at the streamwise location of x = 0.43 m. The sensor had a wire of 5 μm diameter, 1.25 mm length ($l^+ = 416$) an approximate resistance of 3.5 Ohms, and was made out of platinum-coated tungsten. With a large l^+ value there is a likelihood of significant spatial attenuation of the smallest scales, but since it was difficult to obtain measurements very close to the wall due to the high speed of the flow, all of the results represent points in the outer boundary layer and higher. The wire was tuned with an AA Systems anemometer using an over-heat ratio of 1.7. Due to the compressible nature of air in the high-speed region, a modified King's Law approach that accounted for flow densities was used to acquire a time series of velocities from a time series of voltages. For the experimental hot-wire data, a sampling time of 10 s and a sampling frequency of 80 kHz satisfying the Nyquist criterion were used.

An array of 22 XTL/XTEL-140 Series Kulite pressure transducers was placed on the side wall of the wind tunnel at the x = 0.43 m streamwise position. The transducers (kulites) were spaced 7 mm apart, with the first one being 4 mm from the upper wall. The kulites were screwed into place and secured with pressure-fit O-rings such that the kulite face was flush with the inside of the wind tunnel. A sampling time of 15 s at a frequency of 20 kHz was used to acquire time series of fluctuating static pressures.

III. Results

The mean velocities of the flow as a function of position within the wind tunnel for both the forced and unforced cases are plotted in Figure 3. In Figure 3(a), the Y = 0 m. position represents the centerline of the shear layer, a horizontal projection of the splitter plate, with the Y ~ 0.08 m. location representing the upper tunnel wall. The plot resembles a typical shear layer velocity profile with a uniform region of high-speed flow above the shear layer and the turbulent boundary layer clearly present on the upper wall. Static taps were installed across the upper wall to ensure the lack of a streamwise pressure gradient. Figure 3(b) shows the velocity profile recast in boundary layer units, with the boundary layer thickness δ_{99} determined to be 19.7 mm.

The objective of the experiment described in this paper was to attempt to capture with hot-wires the apparent amplitude modulation phenomenon seen in the wavefront data that appeared to occur due to the passing of coherent structures in the forced shear layer. For this reason, the forcing signal sent to the voice coil actuator at the splitter plate was recorded during the acquisition of both unsteady pressure and velocity data. For both the aero-optical and the present hot-wire experiments the two-cycle repeat (harmonic and subharmonic) was used to phase-

lock the optical data in the previous experiment the pressure and turbulence results in the experiment reported here. Rennie et al. [8] demonstrated the ability to robustly force this specific shear layer at high speeds, and more details about the forcing can be found in their paper.

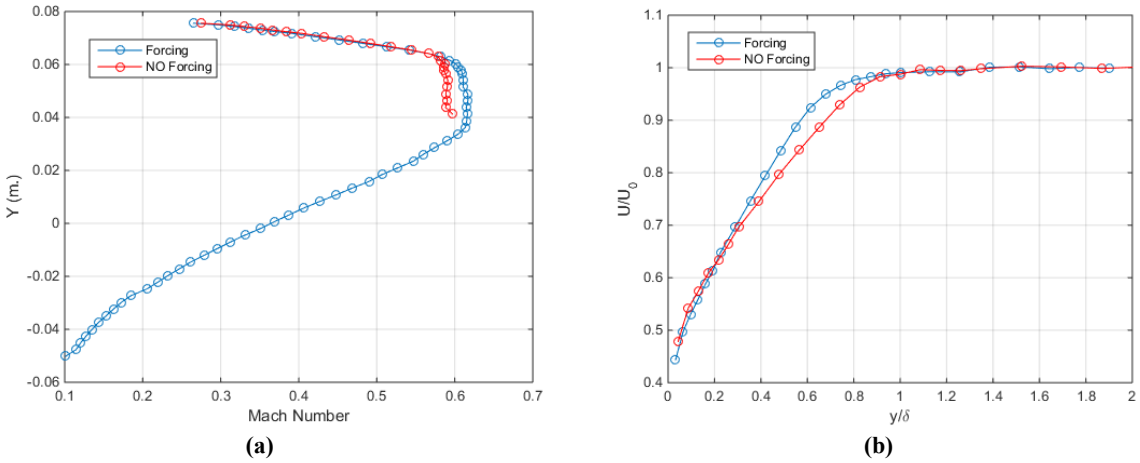

Figure 3. Mean Mach number profile in CSLF (a), represented as velocity in outer units (b)

Figure 4(a) shows two instantaneous pressure "wells" associated with the passing of the forced shear layer coherent structures, and Figure 4(b) shows the phase-locked average of approximately 1,000 instantaneous structures advecting past the measurement plane of the kulites. The discontinuities associated with the instantaneous quantities are found to smooth out in the phase-locked average. The convecting coherent structures create a concomitant unsteady pressure field in the flow; this is experienced in the boundary layer as a variation of the effective freestream velocity.

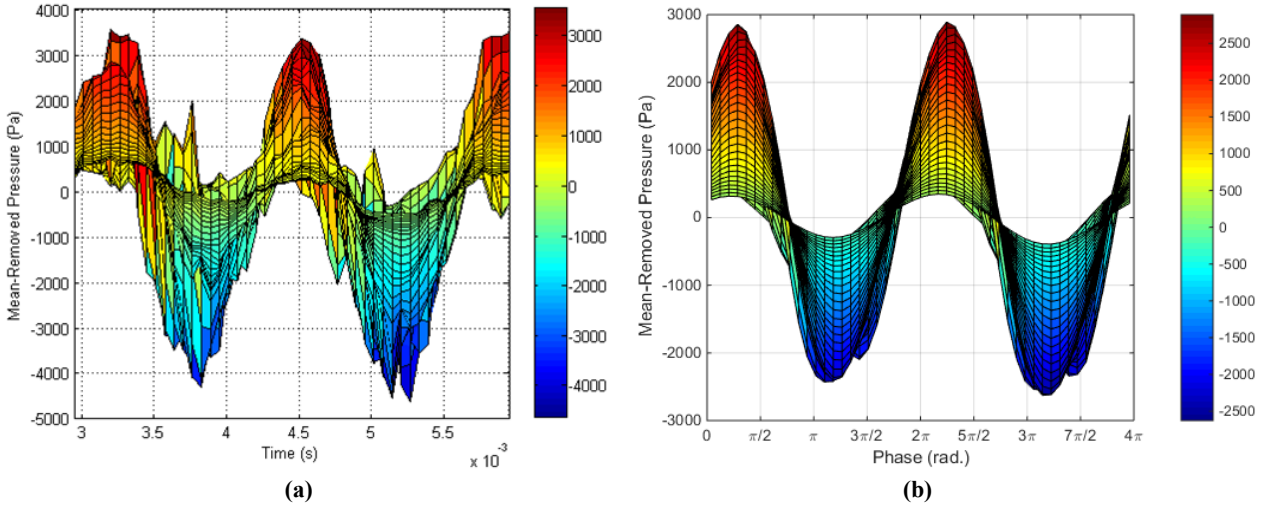

Figure 4. Static pressure, instantaneous (a) and phase-lock averaged (b)

The turbulence intensity, TI, was calculated at each point in the boundary layer by normalizing the RMS of the velocity fluctuations by the free stream velocity. Since the flow was being forced with a sinusoidal signal, the TI of the original time series was not expected to follow and, indeed, did not follow the traditional definition of TI. As such, the forcing frequency was filtered out of the time series of fluctuating velocity. The TI in the boundary layer calculated for both the original time series and the time series with the forcing frequency filtered are shown below in Figure 5, along with the turbulence intensity profile in the case of no active forcing. The production of turbulence near the wall through the work of Reynolds stresses against a mean velocity gradient is evident in the plot. It can be

seen that the CSLF is a relatively quiet wind tunnel, with the freestream turbulence of approximately 1% in the unforced case.

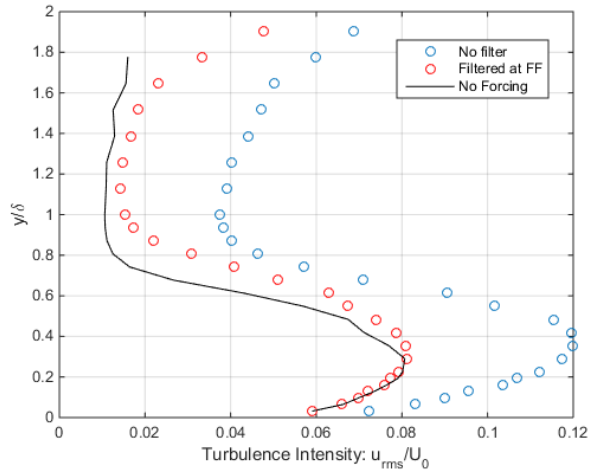

Figure 5. Turbulence intensity profiles in outer scaling units

The time series of velocities were post-processed using the same phase-locking algorithm as the pressures. The original time series without the notch filter at the forcing frequency was phase-locked averaged over the two-cycle forcing signal with the phase range of 0 to 4π subdivided into 50 equally sized bins. An example of a phase-locked velocity time series is shown in Figure 6. In this figure, the blue markers represent the average of all the points in the specific bin representing each phase. The red bars in the left plot of Figure 6 represent the RMS of all of the points in each bin, the average of which is the blue marker which represents the average velocity fluctuation at that phase. The actual magnitude of the turbulence bar at each phase is plotted along with the average velocity fluctuation at that phase in the right plot of Figure 6. The phase-locked velocity fluctuation is sinusoidal with a zero-mean across all phases. This represents one way to validate the phase-locking algorithm, since the mean of the entire time series of velocity fluctuations is also, by definition, zero. Analyzing the turbulence in this manner helped separate the turbulence from the sinusoidal component. The sinusoidal component of the velocity signal due to the voice-coil actuation is represented by the blue markers, and the magnitude of the turbulence "on top" is represented by the red bars on the left or the red markers on the right.

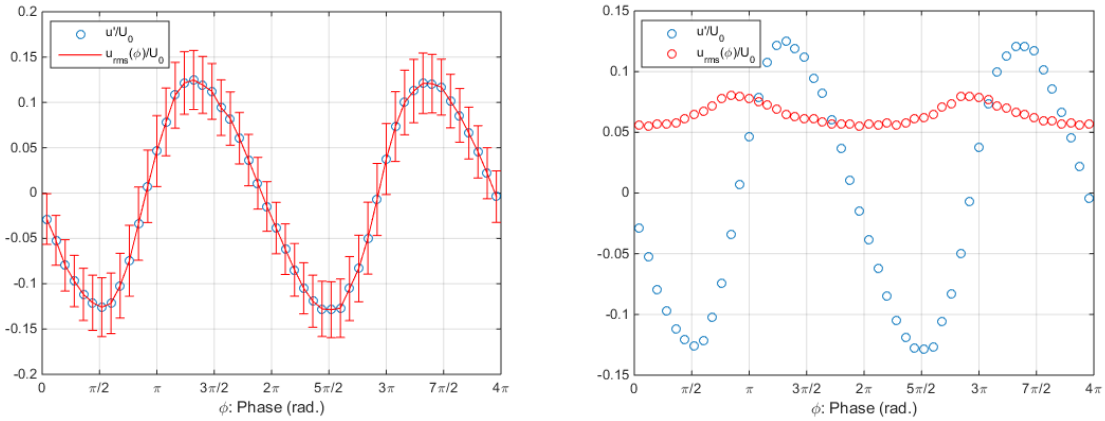

Figure 6. Phase-locked average velocity and turbulence at $y/\delta = 0.355$. Combined (left) and explicitly separated (right)

Figure 6 represents flow at $y/\delta = 0.355$. At this location, there is a marked increase in the magnitude of the filtered TI of the fluctuating phase-locked velocity, which is in turn directly associated with the passing of coherent structures, i.e., it is experiencing amplitude modulation of the turbulence by the externally-imposed large-scale disturbance. The same phase-locked turbulence is plotted for four different wall-normal locations in Figure 7.

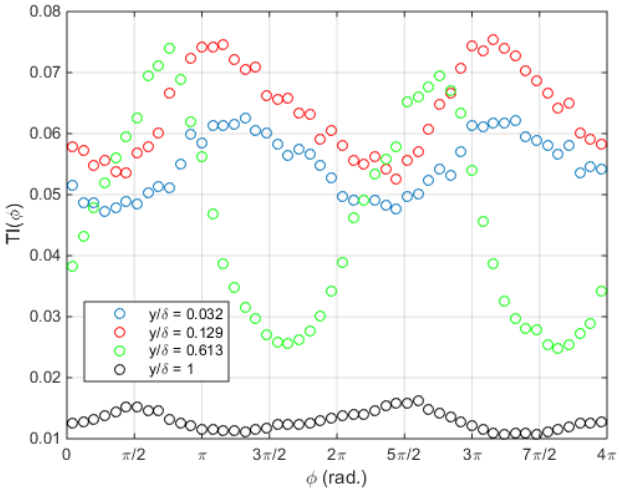

Figure 7. Phase-locked average turbulence at various wall-normal locations

It can clearly be seen from Figure 7 that as the wall-normal location increases, the magnitude of the phase-locked TI increases. For example, at $y/\delta = 0.613$, there is close to a 5% amplitude modulation of the TI. As the wall-normal location increases to a value of $y/\delta = 1$, the magnitude of the turbulence amplitude modulation decreased significantly; although, it is noteworthy that the peak in amplitude is now anti-correlated in phase with the first two locations shown. For each wall-normal location in the boundary layer, the difference between the largest and smallest value of $TI \equiv u_{rms}(\phi)/U_0$ was calculated and will be referred to as the magnitude of the modulated amplitude of the turbulence. As noted above, the phase location of the peak amplitude in the modulation depends on wall-normal location. In the uniform region, for example, the slight modulation occurs closer to $\pi/2$ rad., however closer to the wall at $y/\delta = 0.032$, the modulation occurs at $3\pi/2$ rad., representing a phase jump of nearly π radians. This variation of phase with the peak in modulation activity can be represented through the use of a correlation coefficient as will be shown near the end of the section. The magnitude of the turbulence modulation throughout the boundary layer is plotted in Figure 8. As mentioned earlier, the largest amplitude of the modulation occurs at around $y/\delta \approx 0.4 - 0.8$.

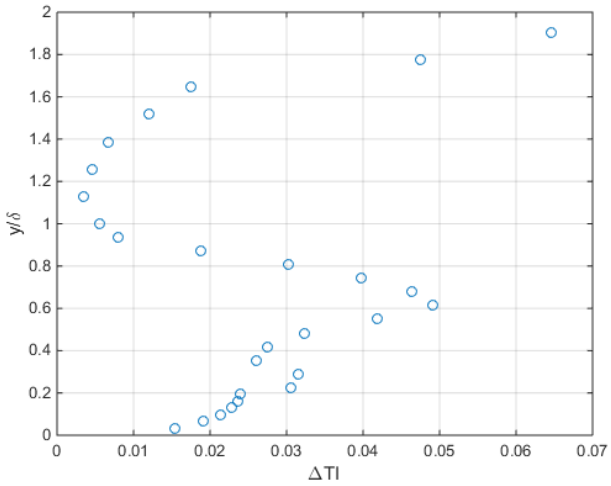

Figure 8. Magnitude of turbulence burst throughout boundary layer

One might be tempted to interpret the turbulence modulation in the context of favorable and unfavorable fluctuations in pressure gradients as a possible rationale for the increased turbulence. Figure 9 combines the velocity and turbulence results, and shows the fluctuating velocity and the RMS of the velocity in each bin normalized by the

free-stream velocity in the high-speed region of the shear layer, and the static pressure fluctuations normalized by the inlet total pressure.

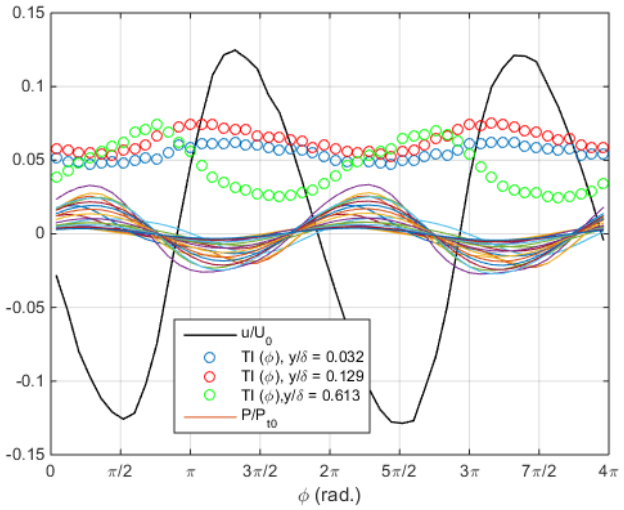

Figure 9. Combined phase-locked average velocity at y/$\delta = 0.355$ (—), phase-locked averaged turbulence intensity at three wall-normal locations (○), and phase-locked averaged pressure at all locations (colored lines).

Figure 9 shows that when the velocity and pressure data are phase-locked over the same two-cycle signal, there is a clear relationship between the two data sets. Regions of high pressure correspond to a negative velocity fluctuation, and regions of lower pressure represent positive velocity fluctuation. The peak amplitude modulation of the turbulence can be seen to occur closer to the leading edge of the disturbance with increasing wall-normal distance, a trend which will be captured in its entirety towards the end of the section. With a high-speed relatively thin turbulent boundary layer, it is difficult to make measurements close to the wall, and since the original motivation for the experiments was to study the turbulent bursts in the optically active portion of the boundary layer observed by Duffin [7], all the hot-wire results represent points in the outer boundary layer.

The entire boundary layer activity can be visualized using phase-locked contour plots to better understand the behavior of the fluctuating velocity modes and the resulting turbulence modulation. The phase-locked velocity fluctuation as shown in Figure 6 was calculated for the entire set of measurements in the boundary layer traverse and the resulting contour plot is shown in Figure 10 (a). The energy contained within the externally-imposed large scale was modeled as $\tilde{u}_{rms}{}^2/U_0{}^2$, where $\tilde{u}_{rms}$ is the phase-locked averaged RMS of the fluctuating velocity component and U_0 is the free-stream velocity, and is plotted as a function of the wall-normal position in Figure 10 (b).

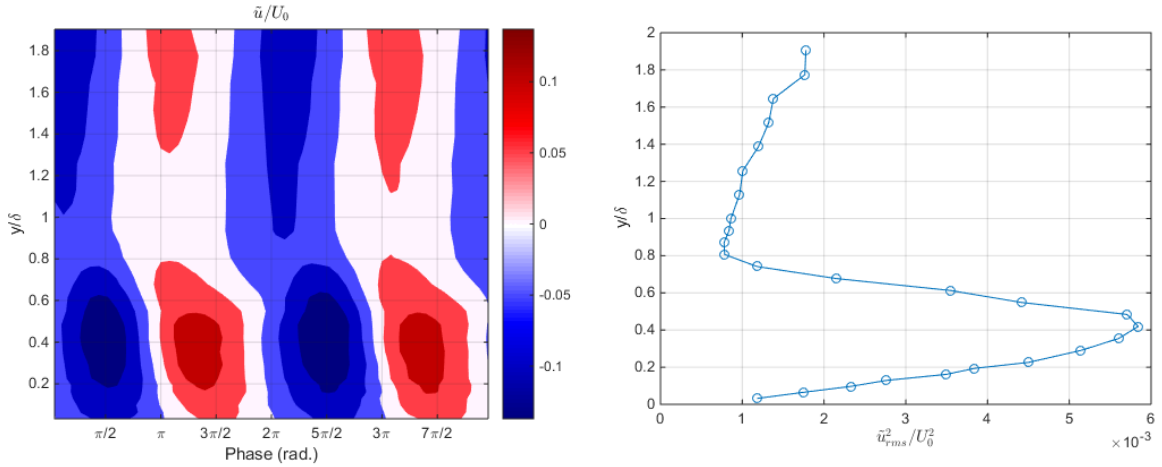

(a) **(b)**

Figure 10. Fluctuating velocity modes (a) and synthetic mode energy (b)

By comparing Figures 9 and 10(a), it can be seen that regions of lower pressure correspond to higher fluctuating velocities and vice versa when phase-locked to the forcing signal. Figure 10 also highlights the deterministic quality of the regularized shear layer. Most of the energy within the modes is concentrated in a region between $y/\delta \approx 0.2 - 0.6$. Figure 10 (b) shows that the peak in synthetic mode energy occurs at a wall-normal location of approximately $y \sim 0.4\,\delta$. From Figure 3(b), it was known that at this location in the boundary layer, the mean velocity is roughly $0.8 \cdot U_\infty$. It is noteworthy that when the contours of fluctuating mass flux were plotted instead of simply the fluctuating velocity, the synthetic mode energy peaked slightly lower in the boundary layer, at a location closer to $y \sim 0.3\delta$ where the mean velocity is roughly $0.7 \cdot U_\infty$.

It is obvious that the work of Duvvuri and McKeon most closely resembles the current work, as in both cases the turbulent boundary layer is excited at a specific forcing frequency and a synthetic large scale is created. Following the work of Duvvuri and McKeon, a spectrogram of the pre-multiplied energy spectra was computed and is shown in Figure 11(a). The spectrogram shows a clear spike at the forcing frequency of 675 Hz. In addition, faint spikes can also be seen at the second and third harmonics, 1350 Hz and 2025 Hz respectively. Notch filters were added at 10 kHz and 20 kHz to filter out non-physical room disturbances. The influence of the second and third harmonics, as well as the subharmonic at 337.5 Hz was studied through a modal decomposition with the use of a bandpass filter around each relevant frequency. This exercise revealed that the fundamental forcing frequency of 675 Hz gave rise to a significant portion of the synthetic mode energy, and thus could be considered to be primarily responsible for the mode shape seen in Figure 10(a).

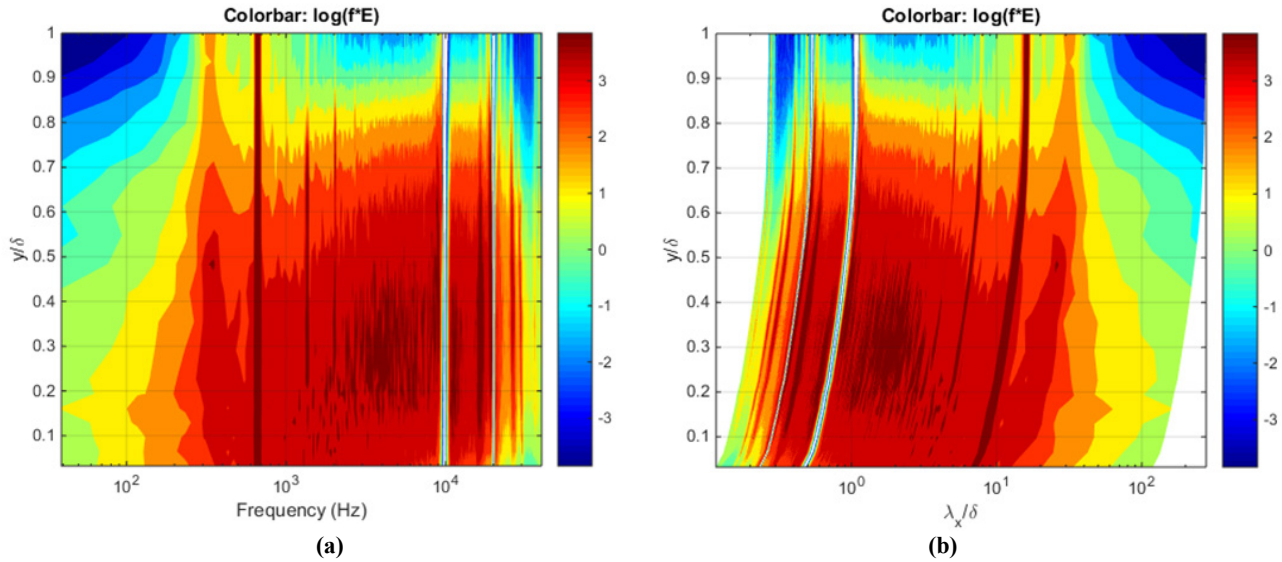

Figure 11. Pre-multiplied energy spectra, frequency (a), wavenumber (b).

The frequency spectrogram was converted to a wavenumber spectrogram using the local mean velocity and Taylor's Hypothesis and is shown in Figure 11(b). The wavenumber spectrogram was used to determine a suitable cutoff criterion to separate the small and large scales following [3]. A criterion of $\lambda_x/\delta = 3$ was chosen to exclude the effect of the second and third harmonics and to best create a correlation between the synthetic scale and the small scales of turbulence.

The amplitude modulation of the turbulence was analyzed using correlation coefficients following the works of Hutchins et al. [5], Mathis et al. [6] and Duvvuri and McKeon [3]. Following [5] and [6], the velocity signal was split into a large-scale and small-scale component using $\lambda_x/\delta = 3$ as the wavenumber cutoff criterion. The concept of modulation of the small scales by the large scales in the flow is described extensively in [6], and the degree of amplitude modulation is represented by R, a single-point modulation correlation coefficient,

$$R = \frac{\overline{u_L^+ \; E_L(u_S^+)}}{\sqrt{\overline{u_L^{+2}}}\sqrt{\overline{E_L(u_S^+)^2}}} \tag{1}$$

where $u_L$and u_S are the large and small scale signal respectively, and E(u_S) represents the envelope of the small scale signal obtained using the Hilbert transform. The coefficient R is computed throughout the boundary layer and is shown in Figure 12.

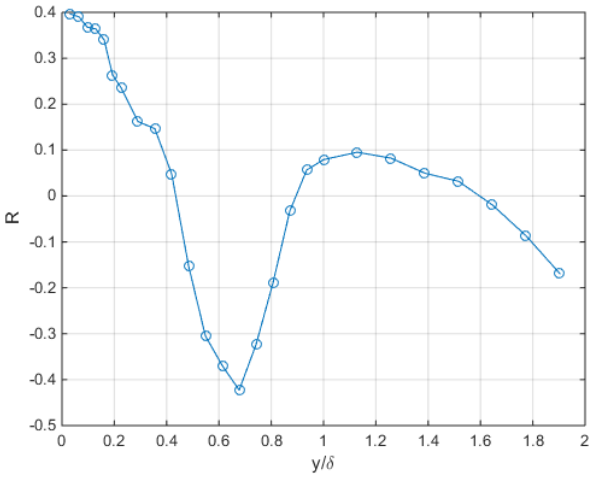

Figure 12. Amplitude modulation correlation coefficient

The modulation coefficient ψ was defined by Duvvuri and McKeon as the correlation coefficient between the sinusoidal component of the velocity due to forcing and the small scale component of the signal, both obtained through phase-averaging with respect to the forcing signal. This coefficient was computed for the turbulent boundary layer forced by the shear layer in the CSLF and is shown in Figure 13.

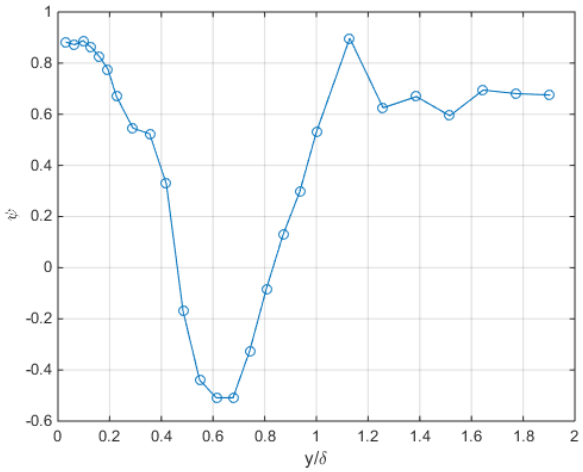

Figure 13. Synthetic scale modulation correlation coefficient

IV. Conclusions

In an attempt to explore what appeared to be turbulence modulation in an aero-optical study of a forced shear layer, a Mach 0.6 turbulent boundary layer was forced using a regularized shear layer which created a concomitant unsteady pressure field that provided a disturbance for the turbulent boundary layer on the upper wall of the tunnel. The apparent turbulence modulation noted in the aero-optical experiment was studied using hotwire anemometry and a phase-locking algorithm to align the results to the deterministic passing of the coherent vortical structures in the shear layer. The phase-locked results were studied in the context of the amplitude modulation effect and were compared with the work of Duvvuri and McKeon [2]. The relationship between the synthetic large scale and the small scales of turbulence in the current work is represented in Figure 13. It was not possible to obtain measurements very close to the wall in the current work. There is sufficient reason to believe that an amplitude

modulation of the small scales by the artificial large scale is what Duffin observed optically with wavefronts. Further testing is in progress to determine the streamwise wavenumber in order to understand why the synthetic mode energy concentrates at a wall-normal location of $y = 0.4\delta$.

Acknowledgments

This effort were funded in part by the High Energy Laser - Joint Technology Office (HEL-JTO) and administered through the Air Force Office for Scientific Research (AFOSR) under Grant Number FA9550-13-1-0001. The U.S. Government is authorized to reproduce and distribute reprints for governmental purposes notwithstanding any copyright notation thereon.

References

[1] Kline, S. J., W. C. Reynolds, F. A. Schraub, and P. W. Runstadler. "The Structure of Turbulent Boundary Layers." *Journal of Fluid Mechanics.* (1967): 741-773.

[2] Jacobi, I., and B. J. McKeon. "Dynamic Roughness Perturbation of a Turbulent Boundary Layer." *Journal of Fluid Mechanics.* (2011): 258-296.

[3] Duvvuri, Subrahmanyam, and Beverley J. McKeon. "Triadic Scale Interactions in a Turbulent Boundary Layer." *Journal of Fluid Mechanics.* 767 (2015)

[4] Bandyopadhyay, Promode R., and A. K. M. F. Hussain. "The Coupling between Scales in Shear Flows." *Physics of Fluids* 27.9 (1984): 2221-2228.

[5] Hutchins, N., and I. Marusic. "Large-scale Influences in Near-wall Turbulence." *Philosophical Transactions of the Royal Society A: Mathematical, Physical and Engineering Sciences*. 365.1852 (2007): 647-664.

[6] Mathis, Romain, Nicholas Hutchins, and Ivan Marusic. "Large-scale Amplitude Modulation of the Small-scale Structures in Turbulent Boundary Layers." *Journal of Fluid Mechanics*. 628 (2009): 311-336.

[7] Duffin, Daniel A. "Feed-Forward Adaptive-Optic Correction Of A Weakly-Compressible High-Subsonic Shear Layer." Dissertation. University of Notre Dame, 2009.

[8] Rennie, Mark, John Siegenthaler, and Eric Jumper. "Forcing of a Two-Dimensional, Weakly-Compressible Subsonic Free Shear Layer." 44th AIAA Aerospace Sciences Meeting and Exhibit (2006)